AEDC-TR-70-1

DYNAMIC CHARACTERISTICS OF A 9-DEG CONE WITH AND WITHOUT ASYMMETRIES AT MACH NUMBER 10

L. K. Ward, Jr. and A. C. Mansfield

ARO, Inc.

March 1970

VON KÁRMÁN GAS DYNAMICS FACILITY
ARNOLD ENGINEERING DEVELOPMENT CENTER
AIR FORCE SYSTEMS COMMAND
ARNOLD AIR FORCE STATION, TENNESSEE

NOTICES

When U. S. Government drawings specifications, or other data are used for any purpose other than a definitely related Government procurement operation, the Government thereby incurs no responsibility nor any obligation whatsoever, and the fact that the Government may have formulated, furnished, or in any way supplied the said drawings, specifications, or other data, is not to be regarded by implication or otherwise, or in any manner licensing the holder or any other person or corporation, or conveying any rights or permission to manufacture, use, or sell any patented invention that may in any way be related thereto.

Qualified users may obtain copies of this report from the Defense Documentation Center.

References to named commercial products in this report are not to be considered in any sense as an endorsement of the product by the United States Air Force or the Government.

DYNAMIC CHARACTERISTICS OF A 9-DEG CONE WITH AND WITHOUT ASYMMETRIES AT MACH NUMBER 10

L. K. Ward, Jr. and A. C. Mansfield
ARO, Inc.

FOREWORD

The work reported herein was sponsored by Headquarters, Arnold Engineering Development Center (AEDC), Air Force Systems Command (AFSC), under Program Element 62201F, Project 8953, Task 09.

The research program was accomplished by ARO, Inc. (a subsidiary of Sverdrup & Parcel and Associates, Inc.), contract operator of AEDC, AFSC, Arnold Air Force Station, Tennessee, under Contract F40600-69-C-0001. The work was done during the period from November 1, 1968, until June 30, 1969, under ARO Project No. VT5910, and the manuscript was submitted for publication on November 21, 1969.

This technical report has been reviewed and is approved.

David C. Reynolds
1st Lt, USAF
Research Division
Directorate of Plans
and Technology

Harry L. Maynard
Colonel, USAF
Director of Plans
and Technology

ABSTRACT

Wind tunnel tests were conducted at Mach number 10 on a 9-deg half-angle cone model using a unique dynamic stability balance having three angular degrees of freedom. Data obtained at $Re_{\ell} = 1.97 \times 10^6$ on models having different types of compound asymmetries have revealed vast differences in the developed motion. A model with a center-of-gravity offset and a small, out-of-plane nose slice as the second asymmetry was found to have a totally unexpected type of instability. The instability was the rapid divergence of the precession arm caused by a Magnus-type moment resulting from an out-of-plane force generated by the nose slice. When the slice was removed (sharp nose model) and the second asymmetry applied by using a small tab at the base, the classical roll resonance was found.

CONTENTS

ILLUSTRATIONS

NOMENCLATURE

A	Reference area (model base area)
C_ℓ	Rolling-moment coefficient, rolling moment/$q_\infty Ad$
C_{ℓ_p}	$\partial C_\ell / \partial (Pd/2V_\infty)$
C_M	Pitching-moment coefficient of a model which has triagonal or greater symmetry (independent of model roll orientation), pitching moment/$q_\infty Ad$
$C_{M_{p\alpha}}$	$C_{M_{p\alpha}} = C_{m_{p\beta}} = C_{np\alpha}$, Magnus-moment coefficient
C_{M_q}	$C_{M_q} = C_{m_q} = C_{n_r}$, damping-in-pitch derivative coefficient
$C_{M_{\dot\alpha}}$	$C_{M_{\dot\alpha}} = C_{m_{\dot\alpha}} = -C_{n_{\dot\beta}}$, damping-in-pitch derivative coefficient
C_{M_α}	$C_{M_\alpha} = C_{m_\alpha} = -C_{n_\beta}$, slope of the pitching-moment coefficient curve
C_m	Pitching-moment coefficient, pitching moment/$q_\infty Ad$
$C_{m_{p\beta}}$	$\partial^2 C_m / \partial (Pd/2V_\infty) \partial \beta$
C_{m_q}	$\partial C_m / \partial (qd/2V_\infty)$
C_{m_α}	$\partial C_m / \partial \alpha$
$C_{m_{\dot\alpha}}$	$\partial C_m / \partial (\dot\alpha d/2V_\infty)$
C_n	Yawing-moment coefficient, yawing moment/$q_\infty Ad$
$C_{n_{p\alpha}}$	$\partial^2 C_n / \partial (Pd/2V_\infty) \partial \alpha$
C_{n_r}	$\partial C_n / \partial (rd/2V_\infty)$
C_{n_β}	$\partial C_n / \partial \beta$
$C_{n_{\dot\beta}}$	$\partial C_n / \partial (\dot\beta d/2V_\infty)$
d	Reference length (maximum model diameter, Fig. 3)
I	Transverse moment of inertia
I_X	Axial moment of inertia
$\tilde{K}_{n,\,p,\,t}$	Nutation, precession, and trim complex modal vectors
ℓ	Model projected length (Fig. 3)
M_∞	Free-stream Mach number
P	Roll rate

q	Pitch rate
q_∞	Free-stream dynamic pressure
Re_ℓ	Free-stream Reynolds number based on model projected length
r	Yaw rate
t	Time
t_m	Mean time
V_∞	Free-stream velocity
XYZ	Body coordinates (Fig. 2)
$\hat{X}\hat{Y}\hat{Z}$	Nonrolling body coordinates (Fig. 2)
$X_T Y_T Z_T$	Tunnel fixed coordinates (Fig. 2)
z_{cg}	Displacement of the model center of gravity from the axis of symmetry along the Z axis (Fig. 3)
$\hat{\alpha}$	Angle of attack relative to the nonrolling coordinates
α_T	Total angle of attack ($\alpha_T \cong \arcsin \tilde{\xi}$)
α_{pt}	Component of the total trim angle which acts about the Z axis (Fig. 3)
$\hat{\beta}$	Angle of sideslip relative to the nonrolling coordinates
Θ, Ψ, Φ	Angles of pitch, yaw, and roll (Fig. 2)
$\lambda_{n,p}$	Nutation and precession damping rates
$\tilde{\xi}$	Complex angle of attack ($\beta + i\hat{\alpha}$)
ϕ'	Angle between the plane of the total angle of attack and the XZ body plane (Fig. 3)
ϕ_N	Angular position of the slice relative to the XZ body plane (Fig. 3)
$\omega_{n,p,t}$	Nutation, precession, and trim angular circular frequencies ($\omega_t = \dot{\Phi}$)

SUPERSCRIPTS

$\dot{}$, $\ddot{}$	First and second derivatives with respect to time
~	Complex quantities

SUBSCRIPT

o	Quantity at reference condition

SECTION I
INTRODUCTION

The present work is a continuation of studies at the von Kármán Gas Dynamics Facility (VKF) which are directed toward the understanding of the dynamic motions of slender bodies which have slight asymmetries and three angular degrees of freedom. The experimental wind tunnel data were obtained using a dynamic balance which has a spherical gas bearing as the pivot and allows the model to have three angular degrees of freedom. The tests were conducted at Mach number 10 in the 50-in.-diam Tunnel C (Gas Dynamic Wind Tunnel, Hypersonic (C)) of the VKF at a Reynolds number (Re_ℓ) of 1.97×10^6. Data were obtained on a 9-deg half-angle cone model with two types of compound asymmetries which yielded separate types of instabilities when roll resonance was approached.

SECTION II
APPARATUS AND PROCEDURE

2.1 THREE-DEGREE-OF-FREEDOM DYNAMIC BALANCE

A sketch of the balance assembly is shown in Fig. 1. The balance consists of a spherical gas bearing pivot, a three-axis variable reluctance angular transducer, a model release mechanism, and a model locking device. The spherical gas bearing provides a nearly frictionless pivot which is desirable for dynamic stability testing at hypersonic speeds where it is necessary to minimize tare damping. The variable reluctance angular transducers provide continuous analog signals proportional to the angular displacements Ψ and Θ of the nonrolling axes (Fig. 2) and provide roll rate data. Models can be released from an initially pitched position with an initial roll rate using the displacement arm and arm lock (Fig. 1). Both of these initial conditions can be varied. The rotating arms are used to lock the model at zero angle of attack. The turbine and air jets (Fig. 1) are used to increase or decrease model roll rate when the model is in the locked position. These same air jets, when pulsed together, may be used to induce angular motion.

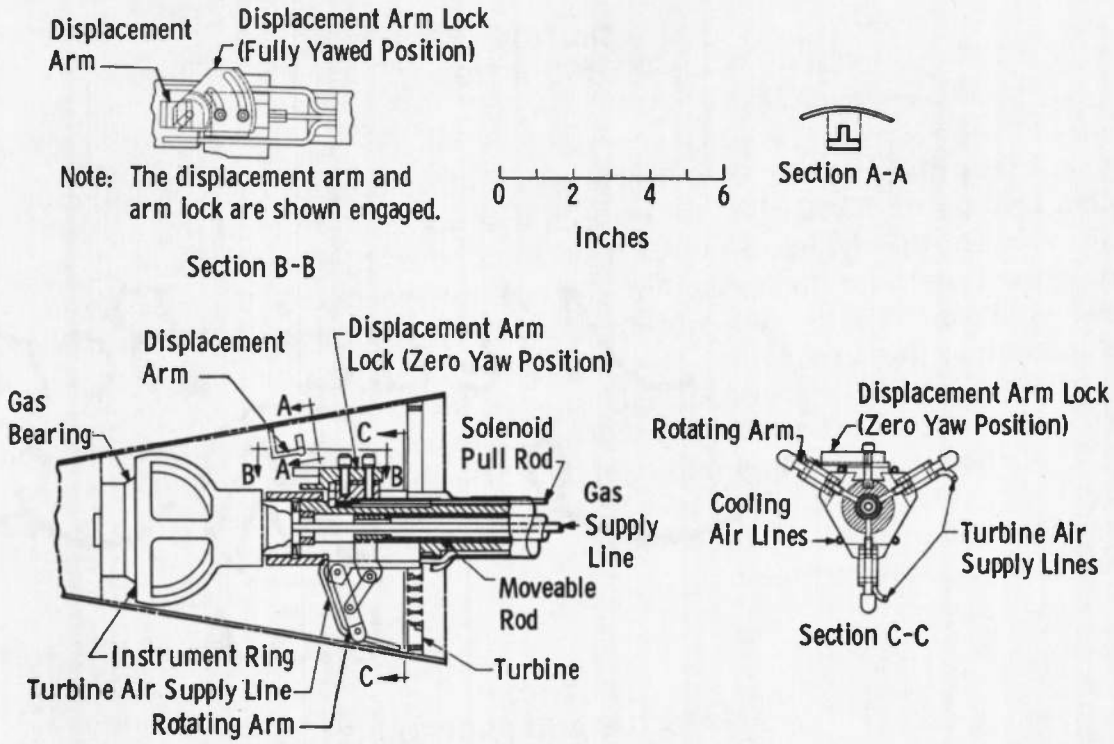

Fig. 1 Balance Assembly

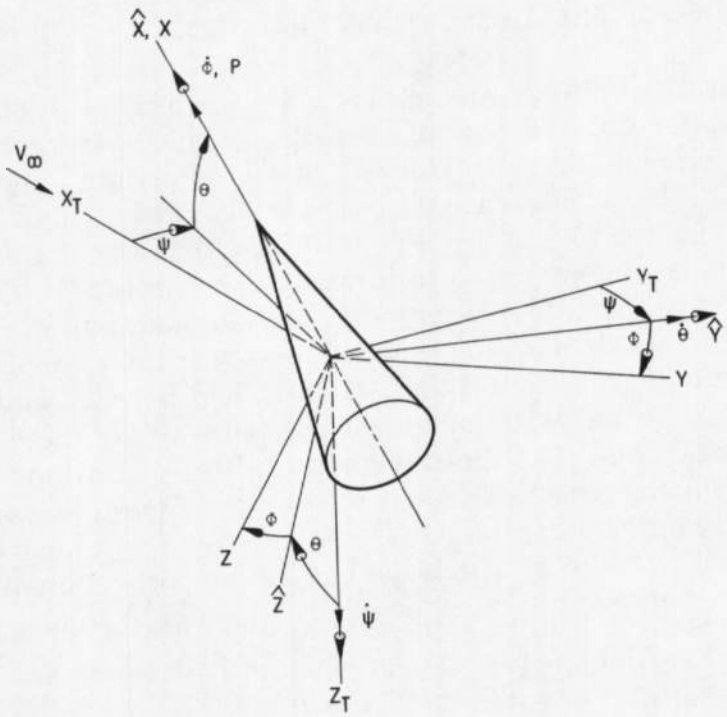

Fig. 2 Coordinate Systems

2.2 MODEL

A sketch of the model used during the tests is shown in Fig. 3. The model was designed such that the pivot point of the balance could be located either on ($z_{cg}/d = 0$) or off ($z_{cg}/d = 0.01065$) the model centerline. The latter provided one asymmetry, and the second asymmetry was provided by adding either a small trim tab at the base or by slicing the nose as shown in Fig. 3. The nose slice angle, θ_N, could be varied through the range θ_N = 0 to 360 deg. The model was dynamically balanced about the XYZ axes, and its center of gravity was coincident with the balance pivot point.

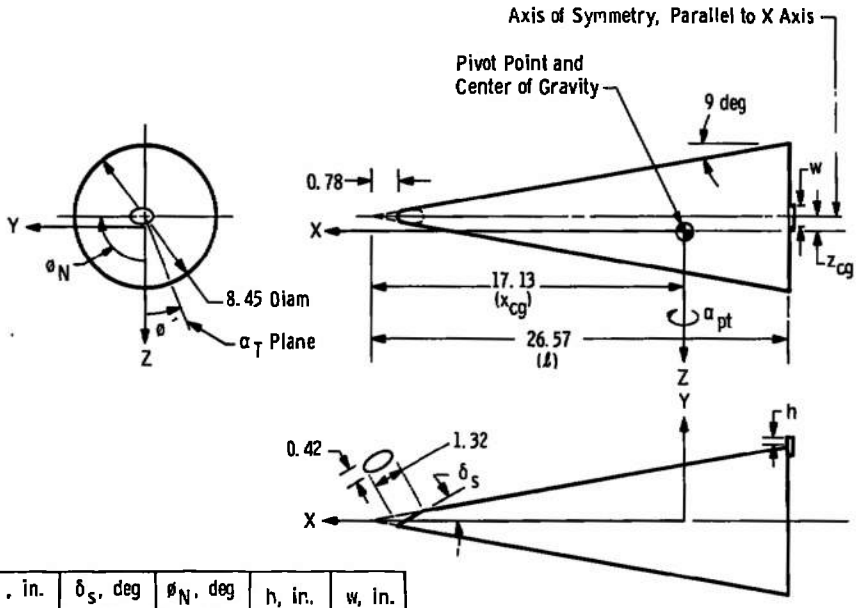

Config.	z_{cg}, in.	δ_s, deg	ϕ_N, deg	h, in.	w, in.
1	0	None	None	0	0
2	0.90	20	270	0	0
3	0.90	20	90	0	0
4	0.90	None	None	0.05	0.75

Fig. 3 Model Geometries

2.3 WIND TUNNEL

Tunnel C is a continuous, closed-circuit, variable density wind tunnel with an axisymmetric contoured nozzle and a 50-in.-diam test section. The tunnel can be operated at a nominal Mach number of 10 or 12 at stagnation conditions from 200 to 2000 psia at 1900°R and from 600 to 2000 psia at 2350°R, respectively. The model may be injected into the tunnel for a test run and the retracted for model cooling or model changes without interrupting the tunnel flow.

2.4 TEST PROCEDURE AND CONDITIONS

The test procedure was to inject the model-balance assembly into the tunnel flow and release the model into motion at the desired initial conditions. After a sufficient amount of data had been obtained, the model was locked and retracted from the flow. While the model was in motion the analog signals from the angular transducers were input directly to an analog-to-digital converter and stored on magnetic tape (a typical example of these data is shown in Fig. 4 where every tenth data point is plotted). The data on magnetic tapes were then input to a CDC 1604-B digital computer for final data reduction.

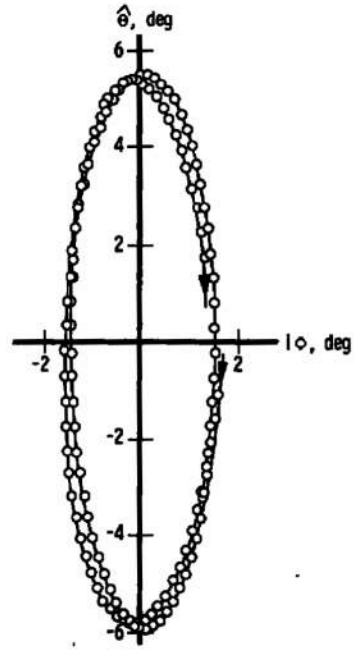

Fig. 4 Typical Data Obtained from Three-Degree-of-Freedom Dynamic Balance

The tunnel and test conditions were as follows:

M_∞	Stilling Chamber pressure, psia	Stilling Chamber temperature, °R	q_∞, psfa	V_∞, ft/sec	$Re_\ell \times 10^{-6}$
10.21	750	1891	154	4764	1.97

The nominal moments of inertia for the test models were as follows:

I, slug-ft^2	Ix, slug-ft^2
0.244	0.0376

SECTION III
METHOD OF DATA ANALYSIS

Data were reduced using the linear tricyclic theory in nonrolling coordinates which was set forth by Nicolaides (Ref. 1). This is the only theory which describes the motion of a rolling, oscillating rigid body in a relatively complete manner. The tricyclic solution (Eq. (3)) was fitted to the displacement-time data obtained from the wind tunnel tests using a data reduction program called "WOBBLE" (Ref. 2), which uses a least-squares differential correction fitting method.

The three-degree-of-freedom equations of motion for a symmetrical rigid body, which include the effects of a small compound asymmetry[1] (Fig. 3), may be written relative to a nonrolling body coordinate system XYZ (Fig. 2) as follows:

$$\dot{P} = \frac{q_\infty Ad}{I_X} C_{\ell_p} [Pd/2V_\infty] + L_0(z_{cg}, \phi', \alpha_T, \alpha_{pt})/I_X \tag{1}$$

$$\ddot{\tilde{\xi}} + [G(t) + iH(t)]\,\dot{\tilde{\xi}} + [J(t) + iK(t)]\,\tilde{\xi} = \tilde{L}(z_{cg}, \phi', \alpha_T, \alpha_{pt})/I \tag{2}$$

where

$$\tilde{\xi} = \hat{\beta} + i\hat{\alpha} = -\psi + i\Theta$$

$$G = -\frac{q_\infty Ad^2}{2V_\infty I}(C_{M_q} + C_{M_{\dot{\alpha}}})$$

$$H = -\frac{I_X}{I} P$$

$$J = -\frac{q_\infty Ad}{I} C_{M_\alpha}$$

$$K = -\frac{q_\infty Ad^2}{2V_\infty I} C_{M_{p\alpha}} P$$

$$\bar{L} = i\tilde{M}_0 \exp(i\,\Phi(t))$$

$$\tilde{M}_0 = q_\infty Ad\,(C_{m_0} + i\,C_{n_0})$$

$$\Phi = \int_0^t P\,dt \qquad \text{(for } P \gg \Psi \sin\Theta\text{, see Fig 2)}$$

In deriving Eq. (2), it is assumed that both the principal aerodynamic moments acting on the model and the transverse moments of inertia of the model are independent of roll position (Φ). It has also been assumed that the motion is restricted to small total angles of attack. The present tests were conducted under conditions of constant density and velocity; therefore, the dynamic pressure, q_∞, was constant.

The moments

$$L_0\,(z_{cg}, \phi', \alpha_T, \alpha_{pt}), \text{ and } \bar{L}\,(z_{cg}, \phi', \alpha_T, \alpha_{pt})$$

are a rolling moment and a trim moment which result from slight aerodynamic and mass asymmetries. They are dependent on quantities

---

[1]Compound asymmetry refers to a center-of-gravity offset (z_{cg}, Fig. 3) combined with an out-of-plane (XZ model plane) aerodynamic trim (α_{pt}).

relative to the body fixed coordinates, XYZ. Unlike the trim asymmetry moment, which has a negligible effect on the model motion except at resonance, the roll moment resulting from a configuration asymmetry can produce significant roll acceleration and, thus, be the dominant moment in Eq. (1)(Refs. 3, 4, and 5).

The tricyclic solution is obtained by using the additional restriction that the coefficients of the differential equation of pitching-yawing motion, Eq. (2), remain constant. This assumption reduces Eq. (1) to

$$\dot{P} = 0$$

The tricyclic solution is given as[2]

$$\tilde{\xi} = \bar{K}_n \exp\left[(\lambda_n + i\omega_n)t\right] + \bar{K}_p \exp\left[(\lambda_p + i\omega_p)t\right] + \bar{K}_t \exp(i\dot{\Phi}t) \qquad (3)$$

where

$$\lambda_{n,p} = -\frac{G}{2} \mp \delta \sqrt{\frac{\sqrt{\left[J - \left(\frac{G^2 - H^2}{4}\right)\right]^2 + \left(K - \frac{GH}{2}\right)^2} - \left[J - \left(\frac{G^2 - H^2}{4}\right)\right]}{2}}$$

$$\omega_{n,p} = -\frac{H}{2} \pm \sqrt{\frac{\sqrt{\left[J - \left(\frac{G^2 - H^2}{4}\right)\right]^2 + \left(K - \frac{GH}{2}\right)^2} - \left[J - \left(\frac{G^2 - H^2}{4}\right)\right]}{2}}$$

$$\bar{K}_t = i\frac{\bar{M}_o}{I} \cdot \frac{1}{\left|(\dot{\Phi} - \omega_n)(\dot{\Phi} - \omega_p) + \lambda_n \lambda_p + i\left[\lambda_n (\dot{\Phi} - \omega_p) + \lambda_p (\dot{\Phi} - \omega_n)\right]\right|}$$

and

$$\delta = \frac{\left|K - \frac{GH}{2}\right|}{K - \frac{GH}{2}}$$

[2]The subscripts n and p, denoting nutation and precession, are used throughout Section III as a convenient notation. The nutation arm is identified after fitting the data as the arm having the largest absolute frequency ($|\omega_n| > |\omega_p|$) and the same rotation direction as the roll rate.

The complex constants, $\tilde{K}_n$ and $\tilde{K}_p$, are determined by the initial conditions. DeMoivre's theorem (Ref. 6) is used to obtain the exact expressions for the modal damping rates ($\lambda_{n,p}$) and circular frequencies ($\omega_{n,p}$).

Once the modal damping rates and frequencies have been determined by the iterative fitting process, the aerodynamic coefficients may be obtained by using the following relations:

$$\left.\begin{aligned} C_{M_q} + C_{M_{\dot{\alpha}}} &= \frac{2\,V_\infty\,I}{q_\infty\,Ad^2}(\lambda_n + \lambda_p) \\ C_{M_\alpha} &= \frac{I}{q_\infty Ad}\,(\omega_n\,\omega_p - \lambda_n\,\lambda_p) \\ C_{M_p\alpha} &= -\frac{2V_\infty\,I}{q_\infty\,Ad^2} \cdot \frac{1}{P}\,(\lambda_n\,\omega_p + \lambda_p\,\omega_n) \end{aligned}\right\} \quad (4)$$

In order to obtain the effective rolling-moment coefficient, C_{ℓ_E}, the total rolling moment (M_X) may be evaluated by simply multiplying the axial moment of inertia times the roll acceleration to obtain

$$M_x = I_X \dot{P}$$

or

$$C_{\ell_T} = \frac{M_x}{q_\infty\,Ad}$$

where C_{ℓ_T} is the total rolling-moment coefficient. The roll-damping-moment coefficient, C_{ℓ_p}, for these experiments was calculated as outlined by Walchner in Ref. 7, and C_{ℓ_E} was then determined as

$$C_{\ell_E} = C_{\ell_T} - C_{\ell_p}\left(\frac{Pd}{2V_\infty}\right)$$

As would be expected, the damping contribution to the total rolling moment was found to be extremely small.

SECTION IV
RESULTS AND DISCUSSION

The symmetrical, sharp-nose model (Config. 1) was first tested at various spin rates corresponding to values of $Pd/2V_\infty$ up to

about 0.0008. Data obtained from these runs are shown in Fig. 5 and show the static and dynamic derivatives to be constant as $Pd/2V_\infty$ is increased from 0 to 0.0008. Shown also in Fig. 5 are the theoretical predictions of C_{M_α} and $C_{M_q} + C_{M_{\dot\alpha}}$. The experimental C_{M_α} agrees quite well with the conical flow field theory, and the damping derivatives are in good agreement with Brong's unsteady flow field analysis (Ref. 8).

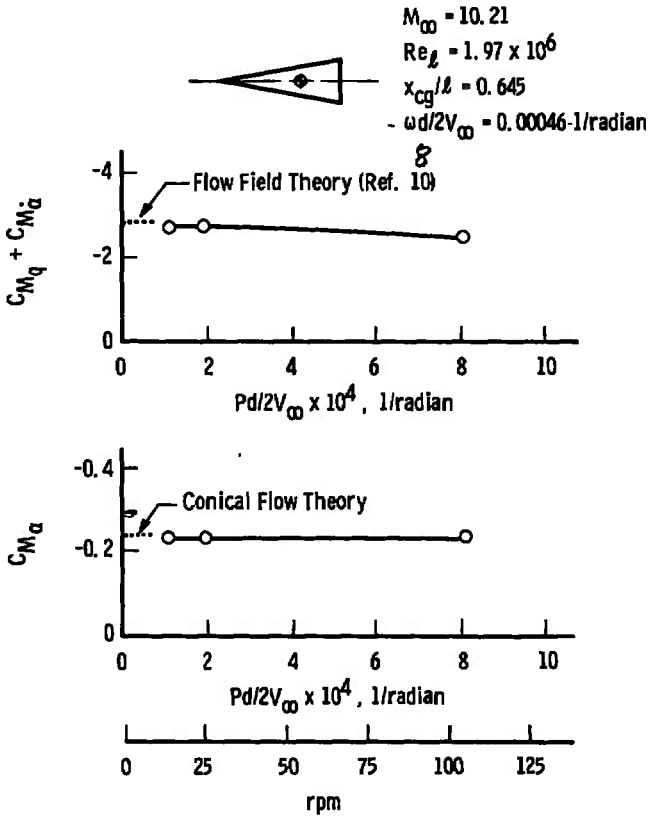

Fig. 5 Variation of the Stability Derivatives with $Pd/2V_\infty$ for the Sharp Nose Symmetrical Model (Config. 1)

Data obtained from Configs. 2 and 3 (the models with compound asymmetries) are shown in Fig. 6. In these figures the magnitudes (K) and rates (ω) of the rotating vectors from the tricyclic solution (Eq. (3)) are shown as a function of mean time. The values plotted are those obtained during the incremental "fitting" of the data and may be thought of as representing the "envelope of the motion." For example, the sum of K_n, K_p, and K_t is the maximum total angle of attack reached during a cycle of oscillation.

Close inspection of the trends of the K's and ω's with time in Fig. 6a reveals two unexpected developments. First, the reader should note that the nose slice is oriented at ϕ_N = 270 deg. Using Fig. 3, one would expect the model to trim with the slice moving into the wind (positive Ψ) and thereby produce a positive side-force coefficient, C_Y, and in turn produce a positive rolling moment (see Eq. (1)) and a positive roll rate. Figure 6a shows the roll rate (ω_t) to be negative. Two independent measurements (static-force measurements and a one-degree-of-freedom gas bearing) of the negative trim angle produced by the slice in this orientation have been made and agree with the value of about -0.1 deg which was calculated from the present data. Newtonian predictions give the trim induced by the slice to be about 0.7 deg. A hypothesis to the cause is given later.

Figure 6a represents data from a model which had three angular degrees of freedom, a compound asymmetry (which would drive $\omega_t > \omega_n$) and which was released at initial conditions approximately equal to zero. One would expect that with these conditions roll resonance would occur. This, in fact, happened at $t_m \approx 190$ sec where $\omega_t = \omega_n$ and K_t began to diverge. These data appeared to behave properly until about t_m = 200 sec when the precession arm (K_p) began to diverge, the trim arm began to damp and the model later "broke out" of persistent roll resonance. This was the second unexpected development. It should be noted that even though K_t began to damp, K_p was diverging quite rapidly and provided a total amplitude ($K_n + K_p + K_t$) divergence.

Figure 6b shows the same type of data with the model nose slice oriented at ϕ_N = 90 deg. The model was released at an angle of attack of about 6 deg with a slightly negative roll rate. The model damped initially, spun through roll reversal and at about t_m = 160 sec the trim arm (K_t) began to amplify. At the same time, however, K_p started to diverge and lock-in never occurred. Note that the same type of instability seen in Fig. 6a was present.

When the model was locked into persistent roll resonance (Fig. 6a) the motion was lunar ($\omega_t = \omega_n$), giving the model a preferred windward meridian, and the center of gravity was on the windward side. The out-of-plane force produced by the asymmetries produces a moment which acts about an axis which is perpendicular to the X axis at the center of gravity and is contained in the plane of the total angle of attack. This moment has the same effect as a Magnus moment; however, it should not be confused with the classical Magnus moment since it is not a result of the Magnus effect. At conditions other than lunar motion, the magnitude of the out-of-plane force will oscillate

and the net effect of the out-of-plane moment is not as great. This may be seen by comparing Figs. 6a and b as the growth of the precession arm (K_p) was more rapid during roll resonance (Fig. 6a). In Fig. 6a the precession arm (K_p) begins to diverge when the model locked into resonance and later reached a level greater than K_t. This caused the elliptical coning motion of the model ($\alpha\beta$ plane) to change from lunar nutational motion to precessional motion.[3] Lunar motion can only exist when the motion is nutational and resonant. When the precession arm (K_p) began its rapid increase, the model "broke out" of resonance (Fig. 6a), and the spin rate (ω_t) decreased in absolute value. As the spin rate became sufficiently far away from the resonant condition, the effect of the oscillating out-of-plane force diminished and then leveled off and began to damp.

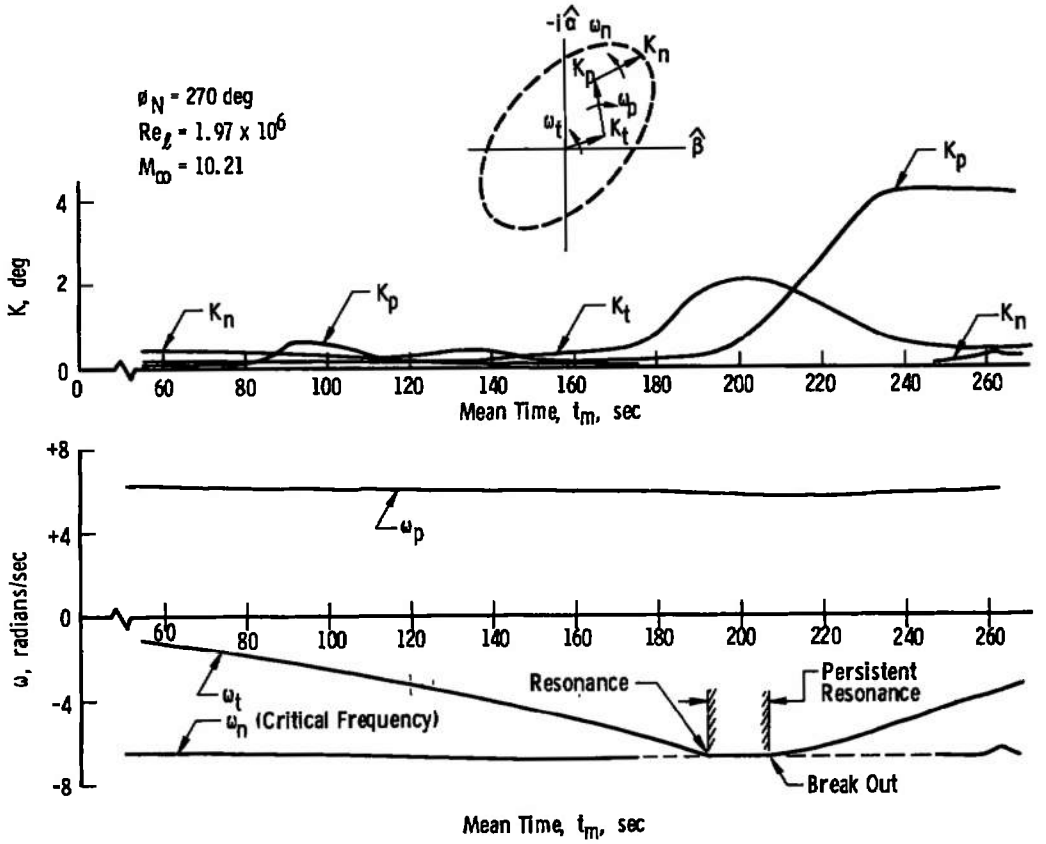

a. Configuration 2

Fig. 6 Trends of the Modal Vectors as a Function of Mean Time

---

[3]Nutational motion ($K_n + K_t > K_p$) is the condition where the coning motion of the model, viewed in the αp plane, has the same direction as the spin rate (ω_t). Precessional motion is the opposite.

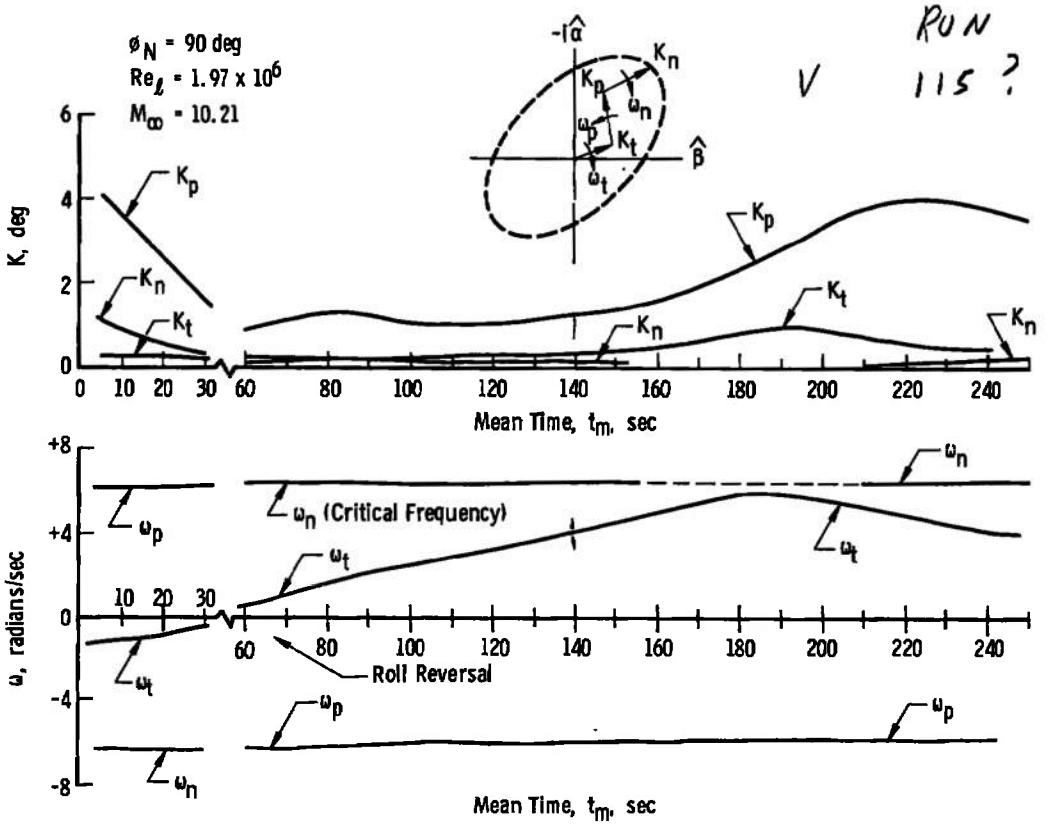

b. Configuration 3
Fig. 6 Concluded

Figure 7 shows the effective rolling-moment coefficient, C_{ℓ_E}, as a function of total angle of attack. The data are shown to indicate both the low level of the coefficient and the nonlinearity implied by the previous figures. During static-force tests conducted using this configuration that were previously mentioned, it was hoped that the rolling moment could be measured as a function of roll position and total angle of attack. These data were inconclusive because of the lack of balance resolution needed to measure the low rolling torque present.

Faced with the realization that the nose slice, which was used as the second asymmetry for the above-mentioned experiments, had not provided the simple roll resonance situation that had been desired, it became apparent to the authors that similar situations could occur with other investigators. For example, those persons working with numerical procedures such as generating trajectories from six-degree-of-freedom computer programs could arbitrarily input a C_{m_0} to produce an aerodynamic trim and get entirely different motion results than the flight vehicle. This is especially true for the case of a vehicle having

an unsymmetrical nose caused by ablation. In addition, the obvious question which arises is, "Why does the slice trim opposite to that predicted by theory?" The answer may be that the slice produces an unsymmetrical flow field and a localized separated region which provides the negative pressure field needed to move the slice away from the wind. A more detailed study is needed to fully answer this question.

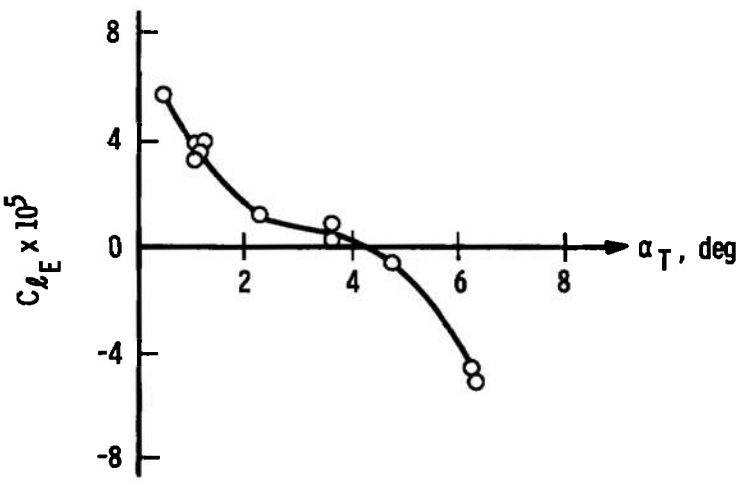

Fig. 7 Rolling-Moment Coefficient as a Function of Total Angle of Attack, Configuration 2, $Re_\ell = 1.97 \times 10^6$

Finally, to compare the motion of models having different types of asymmetries, a sharp nose model with the center-of-gravity offset combined with an out-of-plane trim tab out the base (Config. 4) was tested. These data are shown in Fig. 8b and should be compared with the data in Fig. 8a which are from Config. 3. These later data on Config. 4 show the classical roll resonance. The previous data (Config. 3) show the model motion to be vastly different and demonstrate a type of instability which is felt to be new. This instability, because of its nature, was called a precessional instability.

SECTION V
CONCLUDING REMARKS

Wind tunnel tests were conducted at $M_\infty = 10$ using a dynamic balance having three angular degrees of freedom. Data were obtained at a Reynolds number of 1.97×10^6 on a symmetrical and an unsymmetrical 9-deg half-angle cone model. From an analysis of these data, the following conclusions may be drawn:

1. The dynamic and static derivatives ($C_{M_q} + C_{M_{\dot{\alpha}}}$ and C_{M_α}) were found to be essentially invariant with $Pd/2V_\infty$ (0 to 0.0008 1/radian) for the sharp symmetrical cone.
2. The motion of a model tested with a center-of-gravity offset and an out-of-plane nose slice was found to have a precessional instability which occurred near roll resonance ($\omega_t = \omega_n$) and caused the precession arms to diverge rapidly and damp the trim arm.
3. The motion of a model tested with the center-of-gravity offset and an out-of-plane trim tab at the base was found to develop into that described as classical roll resonance.

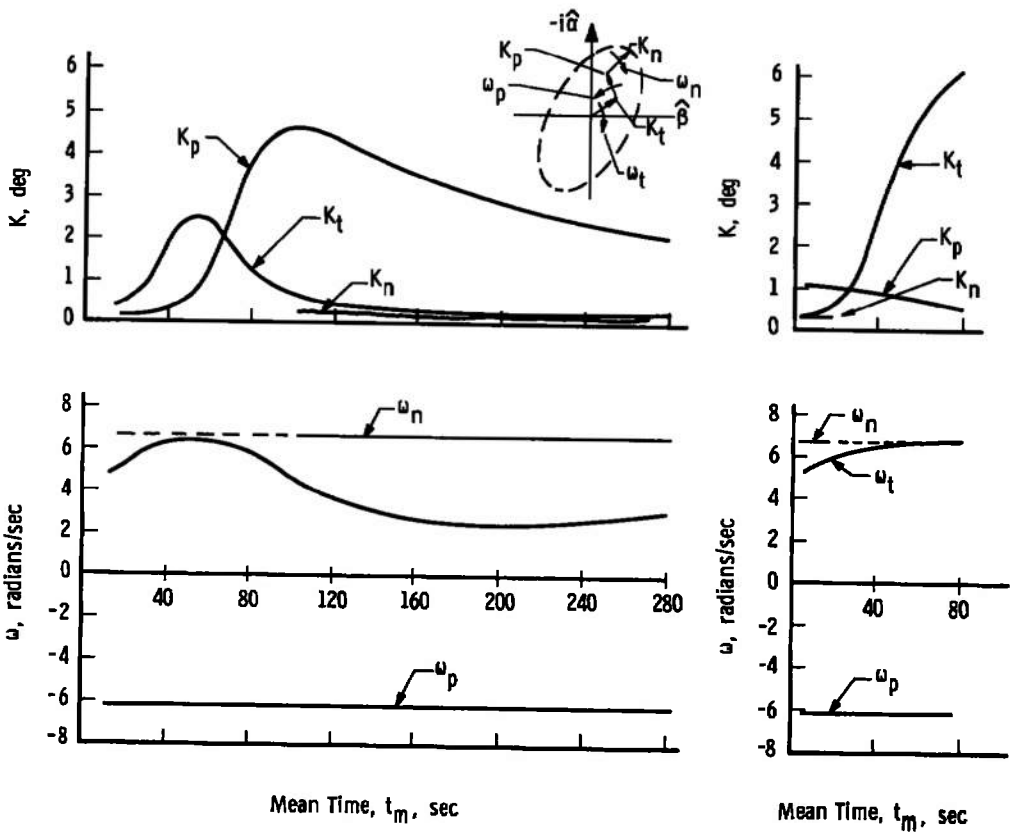

a. Configuration 3

b. Configuration 4

Fig. 8 Comparison of the Modal Vectors of Configurations 3 and 4 as a Function of Mean Time

REFERENCES

1. Nicolaides, J. D. "On the Free-Flight Motion of Missiles Having Slight Configurational Asymmetries." BRL Report 858, June 1953.

2. Nicolaides, J. D. and Eikenberry, R. S. "Dynamic Wind Tunnel Testing Techniques." Paper No. 66-752, AIAA Aerodynamic Testing Conference, September 1966.

3. Vaughn, H. R. "Boundary Conditions for Persistent Roll Resonance on Re-entry Vehicles." Sandia Laboratories, SC-RR-67-287, May 1967.

4. Vaughn, H. R. "Spin-Up and Roll Reversal of Re-entry Vehicle." Sandia Laboratories, SC-RR-68-219, May 1968.

5. Platus, D. M. "A Simple Analysis of Re-entry Vehicle Roll Resonance." SSD-TR-67-25, January 1967. (Aerospace Corporation Report No. TR-1001 (2240-30)-10).

6. Welsh, C. J. and Watt, R. M. "Effects of Roll on the Free-Flight Motion of Statically Stable Bodies." AEDC-TR-67-156 (AD658433), September 1967.

7. Walchner, O. "Laminar Hypersonic Roll Damping Derivatives for a 10 deg Cone." AIAA Journal, Vol. 7, No. 2, February 1969, pp. 342-343.

8. Brong, E. A. "The Unsteady Flow Field about a Right Circular Cone in Unsteady Flight." FDC-TDR-64-148, January 1967.

UNCLASSIFIED

Security Classification

DOCUMENT CONTROL DATA - R & D

(Security classification of title, body of abstract and indexing annotation must be entered when the overall report is classified)

1. ORIGINATING ACTIVITY *(Corporate author)*
Arnold Engineering Development Center
ARO, Inc., Operating Contractor
Arnold Air Force Station, Tennessee 37389

2a. REPORT SECURITY CLASSIFICATION
UNCLASSIFIED

2b. GROUP
N/A

3 REPORT TITLE
DYNAMIC CHARACTERISTICS OF A 9-DEG CONE WITH AND WITHOUT ASYMMETRIES AT MACH NUMBER 10

4. DESCRIPTIVE NOTES *(Type of report and inclusive dates)*
Final Report November 1, 1968 to June 30, 1969

5. AUTHOR(S) *(First name, middle initial, last name)*
L. K. Ward, Jr. and A. C. Mansfield, ARO, Inc.

6 REPORT DATE	7a. TOTAL NO OF PAGES	7b. NO. OF REFS
March 1970	21	8

8a. CONTRACT OR GRANT NO	9a. ORIGINATOR'S REPORT NUMBER(S)
F40600-69-C-0001	
b. PROJECT NO. 8953	AEDC-TR-70-1
c. Task 09	9b. OTHER REPORT NO(S) *(Any other numbers that may be assigned this report)*
d. Program Element 62201F	N/A

10 DISTRIBUTION STATEMENT
This document has been approved for public release and sale; its distribution is unlimited.

11 SUPPLEMENTARY NOTES	12. SPONSORING MILITARY ACTIVITY
Available in DDC.	Arnold Engineering Development Center, AFSC, Arnold Air Force Station, Tennessee 37389

13 ABSTRACT

Wind tunnel tests were conducted at Mach number 10 on a 9-deg half-angle cone model using a unique dynamic stability balance having three angular degrees of freedom. Data obtained at $Re_\ell = 1.97 \times 10^6$ on models having different types of compound asymmetries have revealed vast differences in the developed motion. A model with a center-of-gravity offset and a small, out-of-plane nose slice as the second asymmetry was found to have a totally unexpected type of instability. The instability was the rapid divergence of the precession arm caused by a Magnus-type moment resulting from an out-of-plane force generated by the nose slice. When the slice was removed (sharp nose model) and the second asymmetry applied by using a small tab at the base, the classical roll resonance was found.

DD FORM 1 NOV 65 1473

UNCLASSIFIED

Security Classification

14. KEY WORDS	LINK A		LINK B		LINK C	
	ROLE	WT	ROLE	WT	ROLE	WT
aerodynamic characteristics						
conical bodies						
hypersonic flow						
asymmetry						
stability						